CHAOS Theory and Applications in Applied Sciences and Engineering

e-ISSN: 2687-4539
RESEARCH ARTICLE
Vol.4 / No.3 / 2022 / pp.152-156
https://doi.org/10.51537/chaos.1168824

Numerical Analysis of Semiconductor Ring Lasers with Backscattering Coefficients Mismatch

Nasr Saeed [*,1], **Alain Francis Talla** [α,2], **Alhadji Abba Oumate** [β,3] and **Sifeu Takougang Kingni** [α,4]

[*]Department of Physics, College of Education, Nyala University, P.O. Box: 155, Nyala, Sudan, [α]Department of Mechanical Petroleum and Gas Engineering, National advanced school of Mines and Petroleum Industries, University of Maroua, P.O. Box 46, Maroua, Cameroon, [β]Department of Physics, Faculty of Science, University of Maroua, P.O. Box 814, Maroua, Cameroon.

ABSTRACT The numerical analysis of a semiconductor ring laser (SRL) by using the basic two-mode model and a parameter mismatch in the backscattering coefficients is presented in this paper to account for the asymmetry along the ring. The operation of SRL is discovered to be affected by changing the conservative backscattering parameter for a fixed value of the dissipative backscattering parameter, and the bidirectional regime with alternating oscillation can be suppressed. The numerical results of this paper and the experimental results of the literature depicts a good correspondence.

KEYWORDS
Semiconductor ring laser
Parameter Mismatch
Backscattering parameter
Oscillations

INTRODUCTION

Semiconductor ring lasers are particularly well suited for monolithic integration because, unlike integrated lasers of the Fabry-Perot type, they do not require cleaved facets or gratings to provide the essential optical feedback (M. Sorel and Donati 2002; M. Sorel and Laybourn 2002; T. Krauss and Roberts 1990). Key elements of photonic integrated circuits are SRLs. Due to the active cavity's circular design, a SRL can function in either the clockwise (CW) or counterclockwise (CCW) directions (CCW). For applications such as wavelength filtering, multiplexing-demultiplexing, electrical and all-optical switching, and bistable optical memory, SRLs are potential possibilities (J. J. Liang and Ballantyne 1997). For the investigation of generalized rings and two-mode laser systems, many theoretical models with an emphasis on the interaction between two counter-propagating modes and their interaction with the active medium have been developed. The He-Ne ring laser (Menegozzi and Lamb 1973) and the CO2 laser (H. Zeghlache and Mello 1988) are the systems that have received the most attention, as they were able to take advantage of the rotation-induced asymmetry between the two counter-propagating modes.

In the case of two-mode semiconductor lasers, Etrich et al. (C. Etrich and Zeghlache 1992) have proposed a model based on the time evolution of the electric fields. They discussed how the two counter-propagating modes' interference caused a slowly fluctuating carrier-induced grating that had an impact on how the device operated. In other studies, the formation of intensity oscillations brought on by mode-to-mode phase-coupling is highlighted (R. C. Neelen and Woerdman 1992; P. Mandel and Otsuka 1993; P. A. Khandokhin and Mande 1995). A particular treatment was devised for the SRL by Sargent et al. (Sargent 1993) who derived a simple model for the intensities of the two modes starting from first principles, enlightening the importance of the self- and cross-gain saturation parameters. Later, Sorel et al. (M. Sorel and Donati 2002) proposed a model which takes into account self- and cross-gain saturation effects as in the work of Sargent (Sargent 1993) and includes backscattering contributions originating at the coupling to an output waveguide.

An oscillating bidirectional regime in SRLs was experimentally observed, and this model, which is based on two mean-field equations for the counter-propagating modes and a third rate equation for the carriers, has been successful in explaining this finding. By studying optical switching has been found to be helpful as well (T. Perez and Mirasso 2007) However, as shown by the experimental data, it has not been able to explain the discrepancy in the intensities of the two counter-propagating modes observed in the bidirectional continuous wave (bi-cw) and bidirectional with alternate oscillations (bi-AO) regimes (M. Sorel and Donati 2002; M. Sorel and Donat 2003).

Manuscript received: 31 August 2022,
Revised: 14 October 2022,
Accepted: 15 October 2022.

[1] nasrsaeed19@yahoo.com
[2] alainfrancis.aft@gmail.com (**Corresponding Author**)
[3] oumatealhadji.ao@gmail.com
[4] stkingni@gmail.com

In addition some of the experiments made in SRLs (M. Sorel and Laybourn 2002) showed that applying a current bias on the output waveguide contacts affects the laser operation and unidirectional mode can be achieved. To the best of our knowledge, there is not yet a numerical explanation of the above mentioned experimental results. This paper shows that parameter mismatch in the backscattering coefficients explains the experimental results. The remainder of the paper is as follows. Section 2 presents the rate equations of SRLs and the results obtained during the numerical investigation of SRLs under the backscattering coefficients mismatch .Section 3 concludes the paper.

RATE EQUATIONS OF SRLS AND RESULTS

Due to the fact that the two-mode model has represented SRLs as gyroscopes (Numa 2000) and accounted for the noticed alternating oscillation regime in the light-intensity (L-I) characteristics of the SRL (M. Sorel and Donati 2002). So the model used in this paper is built on the fundamental two-mode model but has a mismatched parameter in the dissipative $k_d{}'$ and conservative $k_c{}'$ backscattering coefficients. The ideal symmetry along the ring is actually never achieved in a real system for a variety of reasons, including flaws in the waveguide, output coupler, and scattering centers [1]. The sum of the two counter-propagating waves can be used to represent the overall electric field inside the ring cavity in the single longitudinal mode operation: $E'(x,t) = E_1{}'\mathrm{e}^{-\mathrm{i}(!_0 \mathrm{t}-\mathrm{kx})} + E_2{}'\mathrm{e}^{-\mathrm{i}(!_0 \mathrm{t}-\mathrm{kx})} + \mathrm{cc}$ where $E_1{}'$ and $E_2{}'$ are the mean-field slowly varying complex amplitudes of the electric field associated with the two propagation directions, i.e., mode 1 is CCW and mode 2 is CW; x is the longitudinal spatial coordinate along the ring circumference, assumed positive in the CCW direction and ω_0 is the optical frequency of the selected longitudinal mode. The rate equations are given by (M. Sorel and Donati 2002; M. Sorel and Donat 2003; L. Gelens and Danckaer 2009; S. T. Kingni and Danckaert 2012; S. T. Kingni and Orou 2020).

$$
\begin{aligned}
\frac{dE_1{}'}{dt'} &= (1+i\alpha)[G_n(N-N_0)(1-\varepsilon_s)|E_1{}'|^2 - \varepsilon_c|E_2{}'|^2 - \frac{1}{\tau_p}]E'_1 \\
&- k'_1 E'_1 \qquad (1a)\\
\frac{dE_2{}'}{dt'} &= (1+i\alpha)[G_n(N-N_0)(1-\varepsilon_s)|E_2{}'|^2 - \varepsilon_c|E_1{}'|^2 - \frac{1}{\tau_p}]E'_2 \\
&- k'_1 E'_2 \qquad (1b)\\
\frac{dN}{dt'} &= \frac{J}{el} - \frac{N}{\tau_s} - G_n(N-N_0)(1-\varepsilon_s|E_1{}'|^2 - \varepsilon_c|E_2{}'|^2) \\
&- G_n(N-N_0)(1-\varepsilon_s|E_2{}'|^2 - \varepsilon_c|E_1{}'|^2)\,. \qquad (1c)
\end{aligned}
$$

where $E_{1,2}$ the fields, $N(t)$ the carrier density, α denotes the linewidth enhancement factor accounting for phase-amplitude coupling in the semiconductor medium, G_n the modal gain factor for the two modes, which depending on the semiconductor gain factor, N_0 the carrier density at transparency, ε_s and ε_c are self-and cross-gain saturation coefficients, respectively and τ_p the photon lifetime in the ring cavity. The parameters $k'_{1,2} = k'_{d_1,d_2} + ik'_{c_1,c_2}$ are the complex backscattering coefficient where k'_{d_1,d_2} the parameters and k'_{c_1,c_2} represent the dissipative and conservative components of backscattering respectively. The parameter J, e, l, τ_s represent the injected ring current density, the electron charge, the active layer thickness and the carrier lifetime, respectively. A suitable normalization of equations (1a) to (1c) leads to the following dimensionless form (M. Sorel and Donati 2002):

$$
\begin{aligned}
\frac{dE_1}{dt} &= (1+i\alpha)\left[n\left(1-s|E_1|^2-c|E_2|^2\right)-1\right]E_1 \\
&- (k_{d1}+ik_{c1})\,E_2 \qquad (2a)\\
\frac{dE_2}{dt} &= (1+i\alpha)\left[n\left(1-s|E_2|^2-c|E_1|^2\right)-1\right]E_2 \\
&- (k_{d2}+ik_{c2})\,E_1 \qquad (2b)\\
\frac{dn}{dt} &= \gamma(\mu - n\left(1-s|E_1|^2-c|E_2|^2\right)|E_1|^2 \\
&- n\left(1-s|E_2|^2-c|E_1|^2\right)|E_2|^2)\,. \qquad (2c)
\end{aligned}
$$

with the following rescalings:

$$
\begin{aligned}
& t = \tfrac{t'}{\tau_p};\ E_1 = (G_n\tau_p)^{\frac{1}{2}}E'_{1,2};\ n = G_n(N-N_0)\tau_p; \\
& s = \tfrac{\varepsilon_s}{G_n\tau_s};\ c = \tfrac{\varepsilon_c}{G_n\tau_s};\ \gamma = \tfrac{\tau_p}{\tau_s} \qquad (3)\\
& k_{d1,2} = \tau_p k'_{d1,2};\ k_{c1,2} = \tau_p k'_{c1,2}; \\
& J_0 = \tfrac{el}{\tau_s}N_0;\ J_{th} = \tfrac{el}{\tau_s}\left(N_0 + \tfrac{1}{G_n\tau_p}\right);\ \mu = \tfrac{J-J_0}{J_{th}-J_0}\,.
\end{aligned}
$$

SRL is numerically analyzed by integrating the set of equations (2a) to (2c) with similar values of parameters to those of (M. Sorel and Donati 2002), but assuming that the backscattering coefficients are varied following the general rule: $k_{c_1,d_1} = k_{c_2,d_2} + \sigma_{c,d}$ or $k_{c_2,d_2} = k_{c_1,d_1} + \sigma_{c,d}$ where the values of the backscattering parameters coincide with those used in (M. Sorel and Donati 2002) and $\sigma_{c,d}$ are the mismatch parameters k_{c_2,d_2} or k_{c_1,d_1} in the conservative and dissipative backscattering coefficients, respectively. The authors of (Kenmogne *et al.* 2022, 2021) present the bifurcation diagrams which depict the local maxima of the trajectories of the systems under investigation. While, Figures 1,2,4,5 and 6 are the amplitude curves which present the global maxima of the trajectories of the sets equations (2a) to (2c). Figure 1 illustrates the L-I curves of both modes by using numerical simulation of sets equations (2a) to (2c) obtained for $k_{d_1} = k_{d_2} = 3.27 \times 10^{-4}$; $k_{c_2} = 4.4 \times 10^{-2}$; $\sigma_c = 10^{-3}$ and $k_{c_1} = k_{c_2} + \sigma_c$.

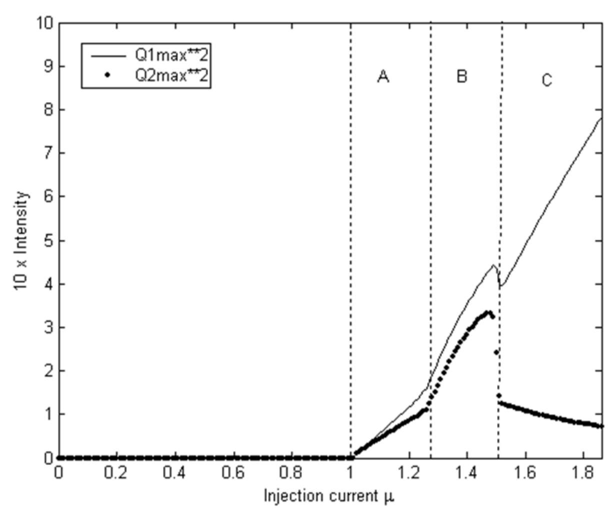

Figure 1 L–I curve for $\alpha = 3.5$, $s = 5 \times 10^{-3}$, $c = 10^{-2}$, $\gamma = 2 \times 10^{-3}$, $k_{d_1} = k_{d_2} = 3.27 \times 10^{-4}$, $k_{c_2} = 4.4 \times 10^{-2}$, $\sigma_c = 10^{-3}$ and $k_{c_1} = k_{c_2} + \sigma$.

When the injection currentμ is increased, Figure 1 exhibits bi-cw (regime A), bi-A0 (regime B) and unidirectional (regime C). Figure 1 shows that $|E_1|^2$ is a bit larger than $|E_2|^2$ in bi-cw and bi-AO regimes as the revealed experimental results of Figure 2.a of (M. Sorel and Donati 2002) whereas in Fig. 2.b of (M. Sorel and Donati 2002) without taking into account the parameter mismatch in the backscattering coefficients, the two modes have the same intensities in regimes A and B. The threshold current in Fig. 2.b of (M. Sorel and Donati 2002) ($\mu_{th} = 1.0$) is equal to the one of Fig. 1 This means that parameter mismatch in the conservative backscattering coefficient does not affect the threshold current in the model. So, one can note that Fig. 1 is more close to the experimental results (see Fig. 2.a of (M. Sorel and Donati 2002)) than Fig. 2.b of (M. Sorel and Donati 2002). Therefore, the mathematical model with parameters mismatch used here is the most indicated way to explain the SRL behaviour. Assuming now $k_{c_2} = k_{c_1} + \sigma$ and $\sigma_c = 10^{-3}$ Figure 2 presents three distinct operating regimes and the same threshold current ($\mu_{th} = 1.0$) as in Fig. 1 but the intensity of CW mode is a bit larger than the intensity of CCW mode.

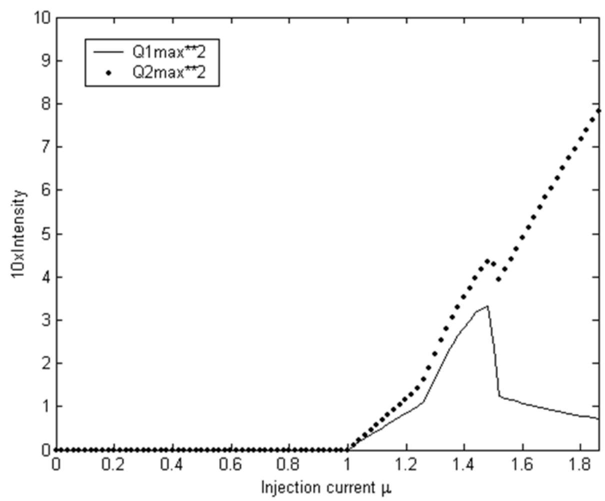

Figure 2 L–I curve for $\alpha = 3.5, s = 5 \times 10^{-3}, c = 10^{-2}, \gamma = 2 \times 10^{-3}, k_{d_1} = k_{d_2} = 3.27 \times 10^{-4}, k_{c_2} = 4.4 \times 10^{-2}, \sigma_c = 10^{-3}$ and $k_{c_2} = k_{c_1} + \sigma_c$.

From Figure 2, one can remark a selection between the two modes according to whether the corresponding mode of is larger or not. The implications of the ring lasing direction when the output waveguide contacts are forward biased, as seen in Figure 3 , are discussed in (M. Sorel and Laybourn 2002), which clarifies this behavior.

According to (M. Sorel and Laybourn 2002) applying bias current I_{W_1} on port 1 larger than 30 mA, the CCW mode is completely suppressed by the increased power sent back into the ring, which also directs the unidirectional laser output to port 2, i.e., on CW mode. This can be seen in Figure 5 of (M. Sorel and Laybourn 2002) , which reports CW power for increasing ring current and for two different bias current values I_{W_1}. Figure 4 presents the L-I curves of both modesobtained for $k_{c_2} = k_{c_1} + \sigma_c$ in order to have the CW mode as a dominating mode.

The numerical findings of this paper and the experimental results of (M. Sorel and Laybourn 2002) are in good accord in Figure 4. To complete this comparison, the L- I curves of both modes are plotted by using the same parameters values as in Fig. 4.

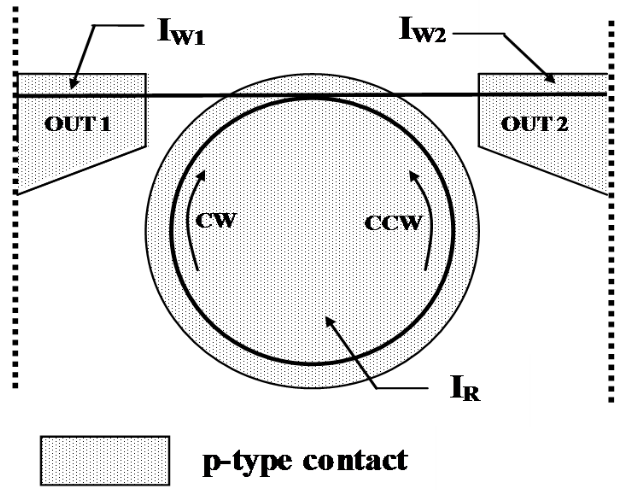

Figure 3 Geometry of ring laser illustrating the layout contact: I_R, I_{W_1}, I_{W_2} indicate the current biases applied to the ring and to the two output waveguide contacts, respectively .

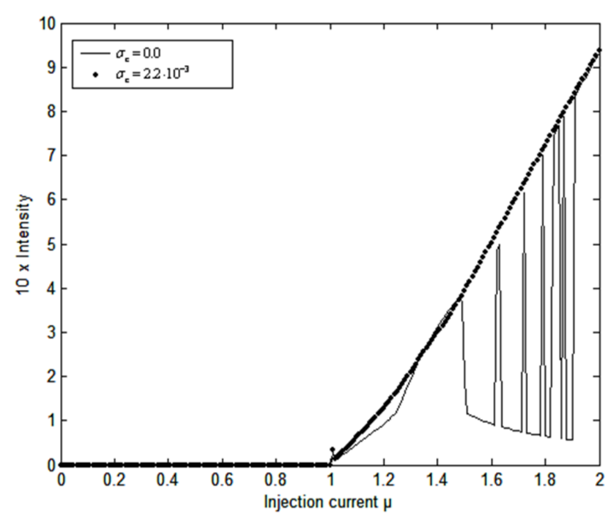

Figure 4 L- I curve of CW mode for $\alpha = 3.5, s = 5 \times 10^{-3}$, $c = 10^{-2}, \gamma = 2 \times 10^{-3}, k_{d_1} = k_{d_2} = 3.27 \times 10^{-4}, k_{c_2} = 4.4 \times 10^{-2}$, and $k_{c_2} = k_{c_1} + \sigma_c$. $\sigma_c = 0$ (solid line) and $\sigma_c = 2.2 \times 10^{-3}$ (dashed line).

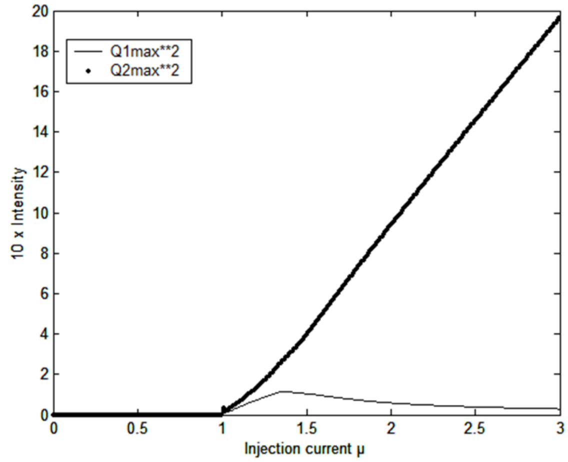

Figure 5 L- I curve of both modes. Parameters values of Figure 4 are conserved.

Figure 5 reveals that for high shift between the two conservative backscattering coefficients, the laser operates only in unidirectional regime. The existing mode is the one having the higher value of conservative backscattering parameters. Fig. 5 also illustrates a good correspondence with the experimental results of Sorel et al. (M. Sorel and Laybourn 2002). Therefore we can note that the experimental correspondence of conservative backscattering parameters $(k_{c_{1},c_{2}})$ can be the current biases applied to the two output waveguide contacts (I_{W_1,W_2}). The higher value of conservative backscattering coefficient of a mode corresponds to lower current bias applied to one of the two output waveguides. The disappearance (or death) of switching observed in Figs. 4 and 5 is sufficient to assert that $(k_{c_{1},c_{2}})$ can be a control parameter for switching phenomenon.

For a fixed value of dissipative backscattering parameter $k_{d_1} = k_{d_2} = 3.27 \times 10^{-4}$, and when varying the conservative backscattering parameter according to $\sigma_c(k_{c_2} = 4.4 \times 10^{-2}$ and $k_{c_1} = k_{c_2} + \sigma$) it is found that the gap between ${Q_1}^2 = |E_1|^2$ and ${Q_2}^2 = |E_2|^2$ modes seen in bi-cw and bi-A0 regimes widens when σ_c is increased. We have also noted by increasing σ_c how the SRL acts to suppress the bi-A0 regime as shown Fig. 6.

In Figure 6, when σ_c is increased, the ${Q_{1,2}}^2 = |E_{1,2}|^2$ in bi-A0 regime narrows progressively. This reduction is due to the decrease of maximum values and the increase of minimum values of each mode simultaneously. In addition, the pump current (μ) interval for the bi-A0 shrinks (see Fig. 6.a to Fig. 6.c) when σ_c is increased and can definitely disappear (see Fig.6.d). Then, we have noted that by increasing σ_c the switching between the two modes is not suppressed, but it is observed just for high value of (μ). Now as the mismatch in the dissipative backscattering is concerned, we have found that using $(k_{c_1} = k_{c_2})$ and $k_{c_1} = k_{c_2} + \sigma$ there is no significant change in the SRL behaviour.

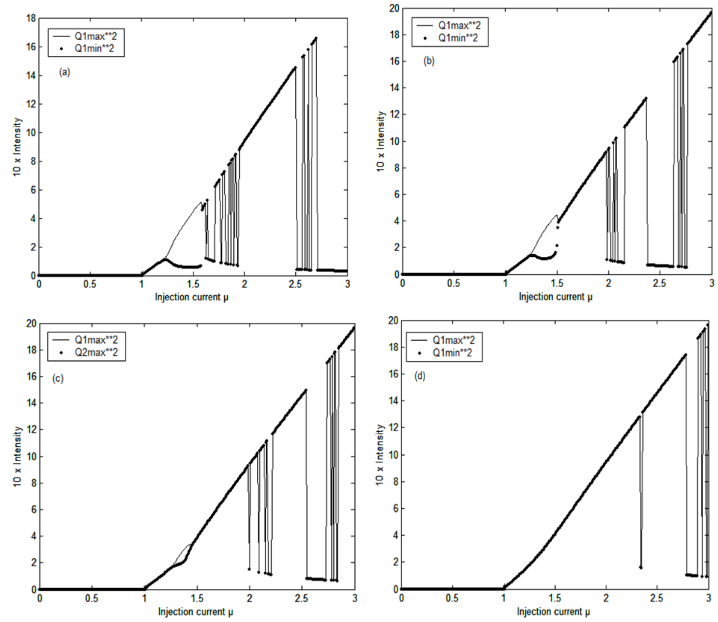

Figure 6 L- I curve of mode 1 displaying the effect of increasing σ_c on the bi-AO regime for $\alpha = 3.5$, $s = 5 \times 10^{-3}$, $c = 10^{-2}$, $\gamma = 10^{-3}$, $k_{d_1} = k_{d_2} = 3.27 \times 10^{-4}$, $k_{c_2} = 4.4 \times 10^{-2}$, $k_{c_2} = k_{c_1} + \sigma$. a) $\sigma_c = 0$; b) $\sigma_c = 10^{-3}$; c) $\sigma_c = 1.7 \times 10^{-3}$ and d) $\sigma_c = 3 \times 10^{-3}$

CONCLUSION

This paper was devoted to the numerical investigation of semiconductor ring laser based on the basic two-modes model with inclusion of a parameter mismatch in the dissipative and conservative backscattering parameters. By varying the conservative backscattering parameter, it was demonstrated that the pump interval for the bidirectional with alternate oscillationsregime shrinks and finally disappears for a given value of the dissipative backscattering parameter. While the difference between the intensities of the two counter-propagating modes were observed in the bidirectional continuous wave and bidirectional with alternate oscillations regimes grows. The mismatch in dissipative backscattering coefficient has no effect on the SRL behaviour. A good correspondence between our numerical resultsof this paper and the experimental results of Sorel et al. (M. Sorel and Donati 2002; M. Sorel and Laybourn 2002) is revealed.

Acknowledgments

S.T.K. is grateful to Professor Paul Woafo (University of Yaounde I, Cameroon) and Doctor Jimmy Hervé Talla Mbe (University of Dschang, Cameroon) for valuable discussions.

Conflicts of interest

The authors declare that there is no conflict of interest regarding the publication of this paper.

Availability of data and material

Not applicable.

LITERATURE CITED

C. Etrich, N. B. A., P. Mandel and H. Zeghlache, 1992 Dynamics of a two-mode semiconductor laser. IEEE J. Quantum Electron **28**: 811–821.

H. Zeghlache, N. B. A. L. M. H. G. L. L., P. Mandel and T. Mello, 1988 Bidirectional ring laser: Stability analysis and time-dependent solutions. Phys. Rev. A **37**: 470–497.

J. J. Liang, M. H. L., S. T. Lau and J. M. Ballantyne, 1997 Unidirectional operation of waveguide diode ring lasers. Appl. Phys. Lett. **70**: 1997–1997.

Kenmogne, F., S. Noubissie, G. B. Ndombou, E. T. Tebue, A. V. Sonna, *et al.*, 2021 Dynamics of two models of driven extended jerk oscillators: Chaotic pulse generations and application in engineering. Chaos, Solitons & Fractals **152**: 111291.

Kenmogne, F., M. L. Wokwenmendam, H. Simo, A. D. Adile, P. M. A. Noah, *et al.*, 2022 Effects of damping on the dynamics of an electromechanical system consisting of mechanical network of discontinuous coupled system oscillators with irrational nonlinearities: Application to sand sieves. Chaos, Solitons & Fractals **156**: 111805.

L. Gelens, S. B., G. Van Der Sande and J. Danckaer, 2009 Phase-space approach to directional switching in semiconductor ring lasers. Phys. Rev. E **79**: 016213.

M. Sorel, A. S. R. M. J. P. R. L., G. Giuliani and S. Donat, 2003 Operating regimes of GaAs-AlGaAs semiconductor ring lasers: experiment and model. IEEE J. Quantum Electron. **39**: 1187–1195.

M. Sorel, A. S. S. B. G. G. R. M., P. J. R. Laybourn and S. Donati, 2002 Alternate oscillations in semiconductor ring lasers. Opt. Lett. **27**: 1992–1994.

M. Sorel, S. D., G. Giuliani and P. J. R. Laybourn, 2002 Unidirectional bistability in semiconductor waveguide ring lasers. Appl. Phys. Lett. **80**: 3051–3053.

Menegozzi, L. N. and W. E. Lamb, 1973 Theory of a Ring Laser. Phys. Rev. A **8**: 2103–2125.

Numa, T., 2000 Analysis of signal voltage in a semiconductor ring laser gyro. IEEE J. Quantum Electron. **36**: 1161–1167.

P. A. Khandokhin, I. K., I. V. Koryukin and P. Mande, 1995 Influence of carrier diffusion on the dynamics of a two-mode laser. IEEE J. Quantum Electron. **31**: 647–652.

P. Mandel, C. E. and K. Otsuka, 1993 Laser rate equations with phase sensitive interactions. IEEE J. Quantum Electron. **29**: 836–843.

R. C. Neelen, D. B., M. P. Van Exter and J. P. Woerdman, 1992 Mode competition in a semiconductor ring laser. J. Mod. Opt. **39**: 1623–821.

S. T. Kingni, L. G. T. E., G. Van der Sande and J. Danckaert, 2012 Direct modulation of semiconductor ring lasers: numerical and asymptotic analysis. JOSA B **29**: 1983–1992.

S. T. Kingni, V. V. T., C. Ainamon and B. C. Orou, 2020 Directly modulated semiconductor ring lasers: Chaos synchronization and applications to cryptography communications. Chaos Theory and Applications **2**: 31–39.

Sargent, M., 1993 Theory of a multimode quasi-equilibrium semiconductor laser. Phys. Rev. A **48**: 717–726.

T. Krauss, P. J. R. L. and J. S. Roberts, 1990 CW operation of semiconductor ring lasers Electron. Appl. Phys. Lett. **26**: 2095–2097.

T. Perez, G. V. d. S. P. C., A. Sciré and C. R. Mirasso, 2007 Bistability and all-optical switching in semiconductor ring lasers. Opt. Express **15**: 12941–12948.

How to cite this article: Saeed, N., Talla, A. F., Oumate, A. A., and Kingni, S. T. Numerical Analysis of Semiconductor Ring Lasers with Backscattering Coefficients Mismatch. *Chaos Theory and Applications*, 4(3), 152-156, 2022.